This is an open access article published under an ACS AuthorChoice License, which permits copying and redistribution of the article or any adaptations for non-commercial purposes.

Langmuir

Article

pubs.acs.org/Langmuir

Cross-Linkable Liposomes Stabilize a Magnetic Resonance Contrast-Enhancing Polymeric Fastener

Cartney E. Smith[†] and Hyunjoon Kong*[,†,‡]

[†]Department of Chemical and Biomolecular Engineering, University of Illinois at Urbana-Champaign, 600 South Mathews Avenue, Urbana, Illinois, 61801 United States

[‡]Institute for Genomic Biology, University of Illinois at Urbana-Champaign, 1206 West Gregory Drive, Urbana, Illinois 61801, United States

Supporting Information

ABSTRACT: Liposomes are commonly used to deliver drugs and contrast agents to their target site in a controlled manner. One of the greatest obstacles in the performance of such delivery vehicles is their stability in the presence of serum. Here, we demonstrate a method to stabilize a class of liposomes that load gadolinium, a magnetic resonance (MR) contrast agent, as a model cargo on their surfaces. We hypothesized that the sequential adsorption of a gadolinium-binding chitosan fastener on the liposome surface followed by covalent cross-linking of the lipid bilayer would provide enhanced stability and improved MR signal in the presence of human serum. To investigate this hypothesis, liposomes composed of diyne-containing lipids were assembled and functionalized via chitosan conjugated with a hydrophobic anchor and diethylenetriaminepentaacetic acid (DTPA). This postadsorption cross-linking strategy served to stabilize the thermodynamically favorable association between liposome and polymeric fastener. Furthermore, the chitosan-coated, cross-linked liposomes proved more effective as delivery vehicles of gadolinium than uncross-linked liposomes due to the reduced liposome degradation and chitosan desorption. Overall, this study demonstrates a useful method to stabilize a broad class of particles used for systemic delivery of various molecular payloads.

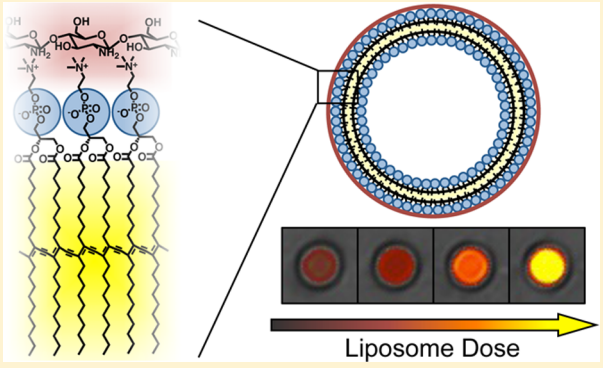

1. INTRODUCTION

Micro- and nanosized liposome particles formed from the self-assembly of lipid molecules have been extensively used to improve the efficacy of diagnostic and therapeutic agents used in various biological applications.[1−3] Specifically, the microstructure, which is morphologically similar to living cells, facilitates encapsulation of various hydrophilic macromolecular drugs within the water-filled core as well as hydrophobic molecules within the lipid bilayer to sustainably release them while extending half-life under physiological conditions. Furthermore, by altering the size, shape, and surface charge, the liposome can tailor biodistribution and efficacy for its particular application.[4−7] In addition, the particle may be conjugated with poly(ethylene glycol) to enhance retention time[8] or ligands to deliver the encapsulated agent to a target site of interest.[9,10] In all, these attributes have allowed for lowered drug dose and reduced toxicity, as well as the capability of diagnostics to probe in vivo microenvironments.

To address various liposomal formulation challenges related to particle functionalization, we recently reported a strategy to modify the liposome surface with functional units (e.g., bioimaging contrast agents) using a polymeric fastener that can associate with both liposome and functional moiety through electrostatic and hydrophobic interactions.[11] This approach offers several advantages over traditional chemical conjugation to the particle surface, often plagued by the inefficiency of surface reactions, laborious and costly purification steps, and hampered molecular self-assembly.[12] Despite the practical advantages of the polymeric fastener, however, the inherent instability of liposomes under in-vivo-like conditions can result in an observed degradation of particles. This was marked by the desorption of the fastener concurrent with a reduction in number of liposomes. Therefore, to stabilize the polymeric fastener, it is strategic to not only stabilize its association with lipids, but to additionally stabilize the liposome itself.

According to previous studies on liposome stability under physiological conditions, liposomal breakdown is caused by any of several mechanisms including osmotic rupture, lipid hydrolysis, and surfactant-induced disintegration.[13,14] Liposomes are also thermodynamically unstable and are prone to aggregation and fusion to reduce their curvature.[15,16] Additionally, serum presents a harsh environment due to degradative enzymes such as serum lipases that can actively digest lipids, as

Received: January 30, 2014
Revised: March 9, 2014
Published: March 17, 2014

 © 2014 American Chemical Society dx.doi.org/10.1021/la500412r | Langmuir 2014, 30, 3697−3704

well as charged proteins that can disrupt electrostatic interactions.[17] The kinetics of such degradation processes are often activated or enhanced at the elevated temperature of 37 °C.

In this study, we hypothesized that cross-linking the lipid bilayer of the liposome following insertion of the polymeric fastener would greatly improve structural integrity of the particle and subsequently retain the desired efficacy of functional units anchored to the liposome surfaces. This hypothesis was examined using diyne lipids to form a cross-linkable liposome and chitosan substituted with octadecyl chains and diethylenetriaminepentaacetic acid (DTPA), a gadolinium chelate, as a model polymeric fastener, termed DTPA-chitosan-g-C_{18}. Their effect on the stability of the chitosan fastener in the presence of serum-supplemented media was examined after anchoring the fastener to the liposome surface followed by cross-linking of diyne lipids via UV irradiation. Finally, the particles were mixed with gadolinium to coat the outer leaflet in order to enhance the quality of magnetic resonance (MR) image contrast. The critical role of cross-linking after adsorption, rather than before, was assessed by thermodynamic analysis. Finally, the functionality of gadolinium-loaded, cross-linked liposome particles after incubation in serum-supplemented media was compared to the non-cross-linked equivalent. The results of this study will be of great benefit in stabilizing liposomes modified with a wide variety of functional moieties through such anchoring.

2. MATERIALS AND METHODS

2.1. Synthesis and Characterization of DTPA-Chitosan-g-C_{18}. All materials were purchased from Sigma-Aldrich unless otherwise noted. Chitosan was coupled sequentially with stearic acid and DTPA through carbodiimide-mediated amide formation as described previously.[11] The product was purified by dialysis (MWCO 6000–8000, Fisher Scientific), lyophilized, and stored as a powder. The degree of substitution of alkyl chain (DS_{C18}) and DTPA (DS_{DTPA}) was quantified by 2,4,6-trinitrobenzene sulfonic acid (TNBS) and xylenol orange assays, respectively.

2.2. Liposome Fabrication. 1,2-Bis(10,12-tricosadiynoyl)-*sn*-glycero-3-phosphocholine ($DC_{8,9}PC$, Avanti Polar Lipids) was dissolved in chloroform at a concentration of 20 mg/mL. During all handling of lipids, samples were protected from light to avoid unintended cross-linking. The lipid solution was transferred to a 50 mL round-bottom flask, and the chloroform was removed by rotary evaporation, leaving a thin lipid film. The film was then hydrated with deionized water at 50 °C to a lipid concentration of 1 mg/mL. Liposomes were then cooled in an ice bath, sonicated for 15 min, and stored at 4 °C.

2.3. Liposome Coating with DTPA-Chitosan-g-C_{18} and Cross-Linking. To coat preformed vesicles, liposomes were incubated in a 0.5 mg/mL solution of DTPA-chitosan-g-C_{18} at a molar ratio of 5:1 glucosamine unit to outer leaflet lipid. To ensure equilibration, the mixture was stirred overnight. Excess chitosan was then removed by centrifugation for 10 min at 4000 rpm to pellet the liposomes. Nonadsorbed chitosan remaining in the supernatant was removed and the coated liposomes were resuspended in deionized water.

Cross-linking of lipids was carried out either before or after binding with modified chitosan. In either case, lipids were cross-linked for 10 min at 4 °C with light at a wavelength of 254 nm (Jelight Co.). Cross-linking was confirmed visually by noting the color change from white to orange.

2.4. Binding Stoichiometry and Stability of Fluorescently Labeled DTPA-Chitosan-g-C_{18}. For quantification, DTPA-chitosan-g-C_{18} was dissolved in deionized water and fluorescently labeled with the amine reactive fluorophore, rhodamine B isothiocyanate, followed by purification by dialysis and lyophilization. Rhodamine-labeled DTPA-chitosan-g-C_{18} was then incubated with liposomes as described. Then, following purification by centrifugation, the fluorescence intensities of the supernatant and resuspended liposomes were analyzed by a microplate reader (Tecan Infinite 200 PRO, Tecan AG, Switzerland) with excitation at 535 nm and emission at 595 nm. Concentrations were determined by quantitation against a calibration curve of fluorescence intensities of known labeled DTPA-chitosan-g-C_{18} concentrations. Binding stoichiometry was then defined as the ratio between bound glucosamine units remaining in the resuspension and outer leaflet lipids.

To examine the stability of the association of DTPA-chitosan-g-C_{18} under biochemically stressed conditions, coated liposomes were resuspended in serum-supplemented media rather than deionized water after removal of excess fluorescent chitosan. Media consisted of 10% type AB human serum off the clot (PAA Laboratories Inc.) in phosphate buffered saline (PBS). Samples resuspended in the serum media were then incubated at 37 °C. At each time point, a sample was removed from incubation and centrifuged for 10 min at 4000 rpm. It was then resuspended and analyzed for fluorescence intensity to determine how much of the initial amount had been desorbed into the supernatant. Background interference from serum, though minimal, was subtracted from the experimental samples for accurate quantitation.

2.5. Thermodynamics of Binding between DTPA-Chitosan-g-C_{18} and Cross-Linkable Liposomes. Isothermal titration calorimetry (ITC) was carried out with a VP-ITC calorimeter (MicroCal, Northampton, MA). Experiments were performed at 25 °C with DTPA-chitosan-g-C_{18} titrated into the 1.45 mL well of liposome suspension. Twenty-eight injections were made over 17.1 s, each with a delay of 300 s between injections. The injection volume was 10 μL and the syringe was stirred at 310 rpm. Analysis was done with Origin 5.0 software from MicroCal using a single-site binding model to determine stoichiometry (N), binding constant (K), and change in enthalpy (ΔH). The initial data point was not included in the analysis.

2.6. Magnetic Resonance Imaging (MRI) of Gadolinium-Loaded Liposomes. To evaluate the MR signal from gadolinium-loaded liposomes under biochemically stressed conditions, the lipid vesicles were incubated with DTPA-chitosan-g-C_{18} as described, followed by removal of free chitosan by centrifugation and addition of $GdCl_3$ to load gadolinium to DTPA binding sites as indicated by xylenol orange assay. Samples were then incubated at 37 °C with 10% serum in PBS. After 1 h, samples were centrifuged again to remove gadolinium-bound DTPA-chitosan-g-C_{18} that was desorbed during incubation. A concentration series was then made using borosilicate cell culture tubes, which were then placed in an agar gel for imaging to immobilize the samples and reduce imaging artifacts. The pH of the liposome suspensions was measured around 7.3 by electronic pH meter (Mettler Toledo, Columbus, OH).

Imaging was completed at room temperature with a 3 T Siemens Magnetom Trio clinical scanner (Siemens AG, Erlangen, Germany). Image acquisition was performed with an inversion recovery turbo spin echo (IR-TSE) sequence with a slice thickness of 3.0 mm, repetition time (TR) of 2500 ms, echo time (TE) of 18.0 ms, and inversion time (TI) ranging from 100 to 1700 ms. For each TI, signal intensity was measured using ImageJ software and used to determine the spin–lattice relaxation time (T_1) of each phantom by nonlinear least-squares curve fitting.

To determine molar relaxivity, the concentration of gadolinium per sample was measured by inductively couple plasma optical emission spectroscopy (ICP-OES, Perkin-Elmer Optima 2000 DV, Norwalk, CT). Prior to analysis, samples were digested in nitric acid to induce sample degradation. Relaxation rate ($1/T_1$) was plotted against gadolinium concentration and relaxivity was determined by linear regression.

2.7. Statistical Analysis. Statistical significance in binding ratios was determined by one-way analysis of variance (ANOVA) with Tukey's HSD test for post hoc pairwise differences. Data was considered significant for $p < 0.05$.

dx.doi.org/10.1021/la500412r | *Langmuir* 2014, 30, 3697–3704

Scheme 1. Chemical Structure of DTPA-Chitosan-g-C_{18} and Its Association with $DC_{8,9}PC$ Liposomes in Three Scenarios: (a) Liposomes without a Cross-Linked Bilayer, (b) Liposomes Cross-Linked before Association with Chitosan, and (c) Liposomes Cross-Linked after Chitosan Anchoring

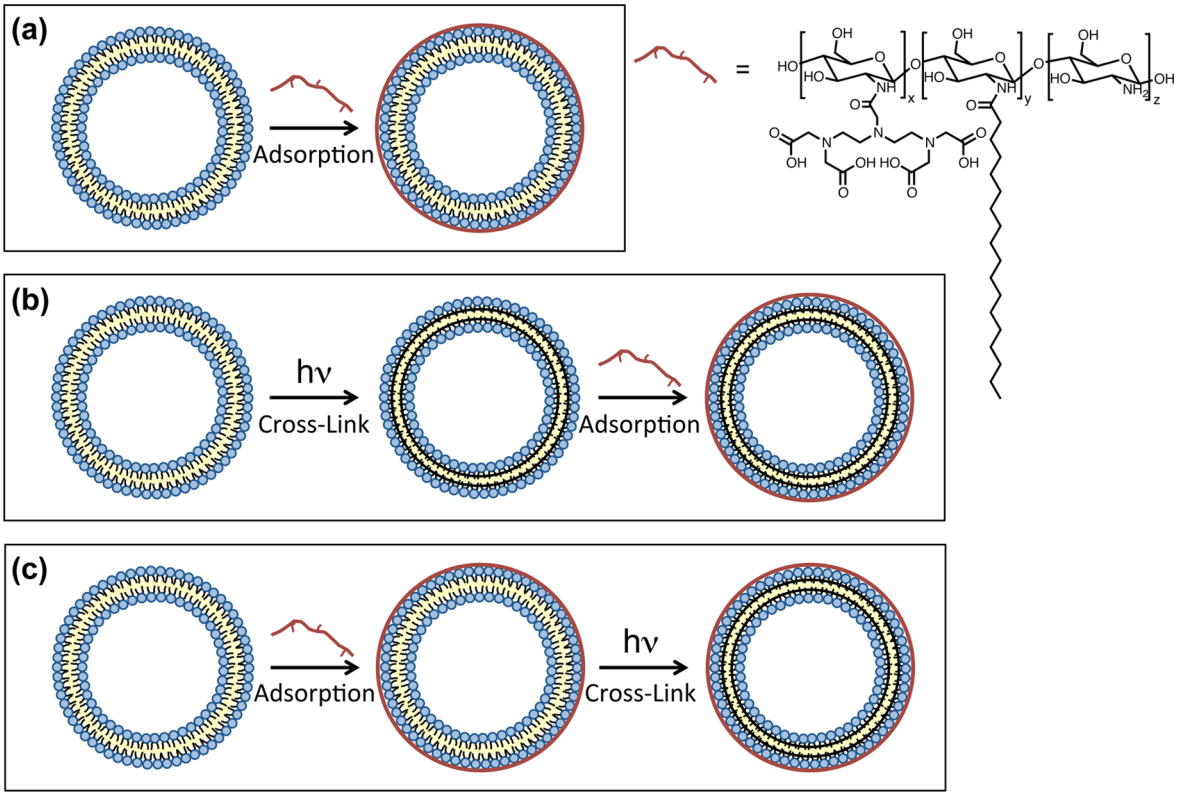

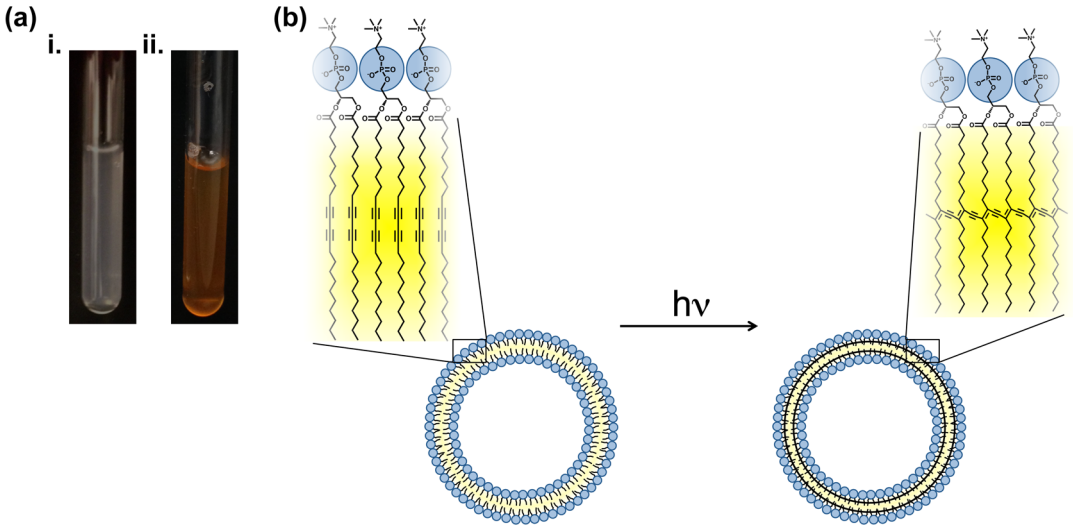

Figure 1. Liposomes with a covalently cross-linked bilayer. (a) Suspensions appear white in color prior to cross-linking (i), but turn orange after exposure to light at 254 nm (ii). (b) Schematic depicting the photoinitiated polymerization of the lipid bilayer.

3. RESULTS AND DISCUSSION

3.1. Formulation of Liposomes Coated with DTPA-Chitosan-g-C_{18}. First, liposomes were formed by film hydration of $DC_{8,9}PC$ lipids. Next, using the fabricated liposomes, we prepared three different systems associated with DTPA-chitosan-g-C_{18} having DS_{C18} of 4% and DS_{DTPA} of 15% (data not shown) by the following methods: (1) incubation of $DC_{8,9}PC$ liposomes with DTPA-chitosan-g-C_{18} (Scheme 1a), (2) exposure of $DC_{8,9}PC$ liposomes to UV light at 254 nm followed by the incubation of the liposomes with DTPA-chitosan-g-C_{18} (Scheme 1b), and (3) incubation of $DC_{8,9}PC$ liposomes with DTPA-chitosan-g-C_{18} followed by exposure to UV light (Scheme 1c). In the second and third processes, the subsequent exposure of the $DC_{8,9}PC$ liposomes to UV light changed the color of the liposome suspension from white to orange (Figure 1a). This color change indicated successful cross-linking between diyne molecules within the bilayer (Figure 1b). The cross-linking reaction had minimal

dx.doi.org/10.1021/la500412r | Langmuir 2014, 30, 3697−3704

effect on the size or morphology of the liposomes (Figure S1, Supporting Information).

3.2. Analysis of DTPA-Chitosan-g-C_{18} Liposome Binding. The binding stoichiometry between DTPA-chitosan-g-C_{18} and liposome, defined as the ratio of glucosamine repeat unit to exposed lipid on the outer leaflet, was further quantified with liposomes associated with rhodamine-labeled DTPA-chitosan-g-C_{18}. Fluorescence intensity of resuspended liposomes and supernatant was measured after centrifugation of the liposome suspension to remove free chitosan and pellet the vesicles. Without the presence of liposomes, DTPA-chitosan-g-C_{18} remained in solution, such that only bound chitosan could be found in a pellet. For the two processes in which the modified chitosan was initially adsorbed to uncross-linked liposomes, the binding stoichiometry was nearly 2.5:1 glucosamine unit-to-exposed lipid (Figure 2). In this way, the process to induce

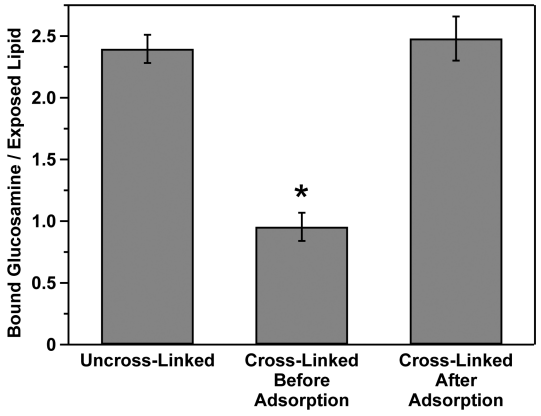

Figure 2. Number of glucosamine units bound per exposed lipid after adsorption to preformed liposomes for the three different formulation conditions. Error bars represent standard deviation of four replicates per condition and an asterisk (*) signifies statistical significance between binding stoichiometries (*$p < 0.05$).

cross-linking between lipids after adsorption of chitosan molecules resulted in a similar binding stoichiometry as chitosan bound to liposomes that were not cross-linked at all. Therefore, the cross-linking reaction of the lipids did not induce desorption of chitosan molecules, nor provide a mechanism of additional adsorption.

Conversely, for the process in which DTPA-chitosan-g-C_{18} was incubated with pre-cross-linked liposomes, the binding stoichiometry was 1:1 glucosamine unit-to-exposed lipid. We suggest that the cross-linked bilayer interfered with the ability of the liposome to bind with chitosan. This may be due to steric hindrance as lipids adopt a rigid conformation that is unfavorable for association between alkyl chains of lipids and those coupled to chitosan. Additionally, cross-linking of lipids likely reduces the fluidity of the lipid membrane, thus impeding the lipids' ability to rotate or translocate for insertion of alkyl chains of chitosan into the bilayer. As we verified previously,[11] insertion of the octadecyl anchors of the fastener plays a critical role in surface binding.

To further understand the thermodynamics underlying the binding between liposome and chitosan, ITC analysis was performed. Liposomes with cross-linked bilayers, as well as those without, were separately titrated with DTPA-chitosan-g-C_{18}. According to the thermograms, it is apparent that the association between liposome and chitosan was endothermic, as indicated by the positive change in heat with each injection of DTPA-chitosan-g-C_{18} (Figure 3). A single-site binding model was applied to extract binding ratios, binding constants, and enthalpies of association.[18]

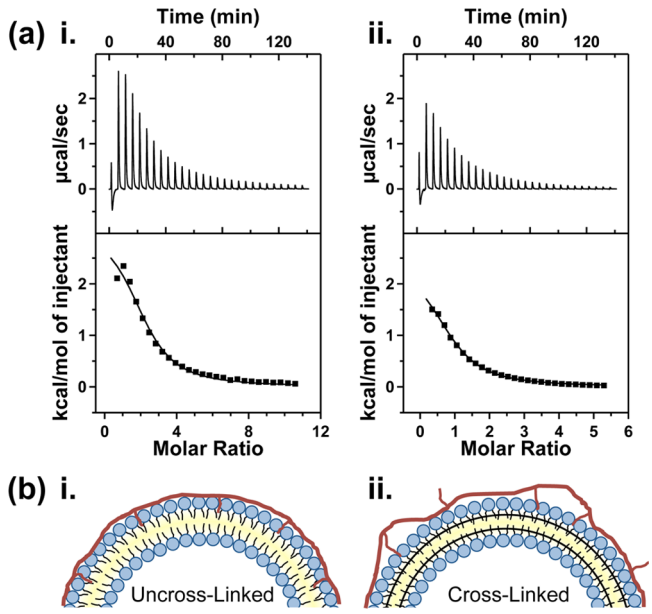

Figure 3. Thermodynamics of binding between DTPA-chitosan-g-C_{18} and liposomes. (a) ITC thermograms comparing the heats of association between DTPA-chitosan-g-C_{18} and liposomes with uncross-linked bilayer (i) or cross-linked bilayer (ii). Heat flow data is shown in the top panel with fitting to a single-site binding model below. (b) Proposed mechanistic explanation of differences in binding energy resulting from the active insertion of alkyl chains into the lipid bilayer (i) and limited insertion of alkyl chains into the pre-cross-linked bilayer (ii).

As in the study described in the previous section, the binding ratio (N) between the glucosamine units and exposed lipids was more than 2-fold greater with uncross-linked liposomes compared to those pre-cross-linked (Table 1). Additionally, the binding constant, K, was greater in the case of uncross-linked liposomes. K was further translated to the change in Gibbs free energy as follows:

$$\Delta G = -RT \ln(K) \quad (1)$$

where T is temperature and R is the universal gas constant. Accordingly, ΔG was negative and greater in magnitude and hence more thermodynamically favorable. It has been previously demonstrated that insertion of a hydrophobic domain into a lipid bilayer contributes to the negative change in ΔG.[19,20] The smaller ΔG associated with cross-linked liposomes suggests that insertion of the 18-carbon anchor of the modified chitosan into the cross-linked liposome is more limited. Therefore, the octadecyl chains of the chitosan likely remain in the aqueous exterior, or insert only partially into the bilayer. In either case, the association of the chitosan with the cross-linked liposome would be weaker than the uncross-linked one.

Additionally, the positive change in enthalpy, ΔH, was smaller when the chitosan was incubated with the cross-linked liposomes. As the change in enthalpy is a sum of various interactions including electrostatic, hydrophobic, and van der Waals forces, as well as hydrogen bonding,[21] the results further

dx.doi.org/10.1021/la500412r | Langmuir 2014, 30, 3697−3704

Table 1. Binding Parameters for the Association between $DC_{8,9}PC$ Liposomes and DTPA-Chitosan-g-C_{18}[a]

liposome	N	K ($\times 10^4$ M^{-1})	ΔH (kcal/mol)	ΔG (kcal/mol)	ΔS (cal/mol·K)
uncross-linked	2.21 ± 0.11	2.04 ± 0.33	3.14 ± 0.22	−5.87	30.2
cross-linked	0.93 ± 0.03	1.34 ± 0.08	2.50 ± 0.10	−5.62	27.3

[a] Molar amounts are listed per mole of glucosamine unit, and error values represent standard deviation of the fit parameters.

indicate a greater level of interaction between the modified chitosan and lipid bilayer when lipids are not confined by cross-linking. The change in entropy, ΔS, was then calculated from the other thermodynamic parameters as follows:

$$\Delta S = \frac{\Delta H - \Delta G}{T} \quad (2)$$

Accordingly, ΔS for the mixture of DTPA-chitosan-g-C_{18} and cross-linked liposomes was smaller in magnitude than that for the modified chitosan complexed with uncross-linked liposomes. Overall, these calculations reveal that the more energetically favorable binding between DTPA-chitosan-g-C_{18} and uncross-linked liposomes was driven by the larger entropic contribution. Consistent with the hydrophobic effect, this entropy-driven process was likely due to the desolvation of water molecules surrounding the hydrophobic alkyl chains of modified chitosan and lipids and the subsequent gain in configurational entropy.[22,23] Therefore, the smaller ΔS in the case of the cross-linked liposomes may again be due to incomplete insertion of the alkyl anchor of the chitosan. Overall, the thermodynamic analysis rationalizes the advantage of incubating DTPA-chitosan-g-C_{18} and liposome suspension prior to the cross-linking reaction of the lipid bilayer for preparation of DTPA-chitosan-g-C_{18} coated liposomes.

3.3. Stability of Liposome Coatings in Serum. The association between liposome and DTPA-chitosan-g-C_{18} was further evaluated in serum-supplemented media. As serum is detrimental to the stability of self-assembled structures in vivo, it was important to assess stability of the chitosan−liposome association in its presence. The percent of DTPA-chitosan-g-C_{18} remaining on the liposome following incubation in serum-supplemented media was determined from the amount of rhodamine-labeled DTPA-chitosan-g-C_{18} liberated from the liposome compared to the amount retained.

In the cases of uncross-linked liposomes and those cross-linked prior to addition of the modified chitosan, more than half of the chitosan was desorbed within 1 h in PBS supplemented with 10% human serum (Figure 4a). There was no statistical difference in the percent desorbed between these two cases. However, when DTPA-chitosan-g-C_{18} was adsorbed to the liposome followed by cross-linking of the lipid bilayer, the retention of chitosan on the liposome was dramatically enhanced ($p < 0.05$). Approximately 75% of the DTPA-chitosan-g-C_{18} that was initially adsorbed remained after 1 h, which was evaluated as a relevant time scale for MRI. Such stable association between DTPA- chitosan-g-C_{18} and liposome continued even after 8 h.

The mechanism of stabilization of the liposome prepared by incubation with chitosan followed by bilayer cross-linking is likely twofold: stabilization of the liposome itself, and stabilization of its association with the modified chitosan. In prior studies, cross-linking of lipids has been shown to improve liposome stability under the stress of surfactant addition.[24] In the present study, the cross-linked lipid bilayer should therefore increase the number of liposomes in the pellet after centrifugation, and consequently the amount of chitosan

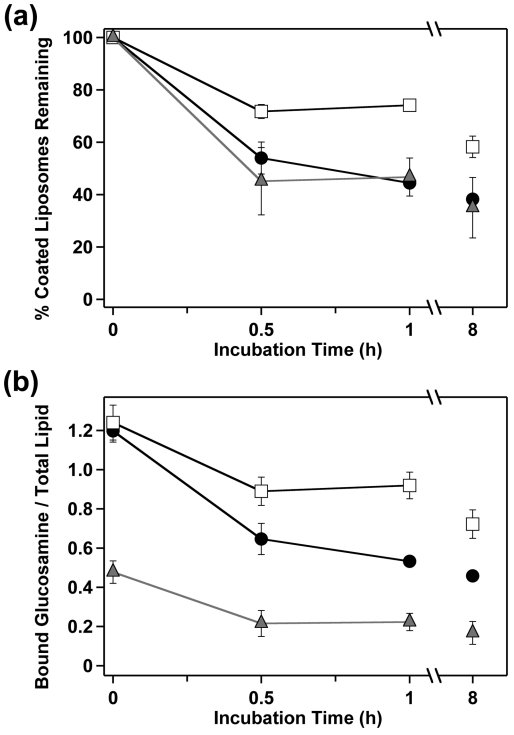

Figure 4. Stability of the association between DTPA-chitosan-g-C_{18} and liposome in serum-supplemented media. (a) Percent remaining of the initial amount adsorbed. (b) Total amount of glucosamine repeat unit remaining, per lipid dose. In (a) and (b), the black filled circle represents the formulation prepared by incubating DTPA-chitosan-g-C_{18} and liposomes without cross-linked bilayer. The gray filled triangle indicates liposomes prepared by incubating DTPA-chitosan-g-C_{18} with pre-cross-linked liposomes. The black open square represents the case of DTPA-chitosan-g-C_{18} incubated with liposomes, followed by cross-linking of the bilayer. Data points and error bars are the average values and standard deviations of three replicates.

quantified in the resuspension versus supernatant. However, dissolution of liposomes cannot be the full picture of stabilization, since there was no difference in the percentage of desorbed chitosan between liposomes cross-linked before chitosan addition and those remaining uncross-linked.

The improved stability of the chitosan−liposome association may also be explained in terms of the adsorption mechanism. Unlike the process to coat cross-linked liposomes, DTPA-chitosan-g-C_{18} incubated with uncross-linked liposomes allowed for complete insertion of the hydrophobic alkyl anchor, thus providing prolonged association with the liposome in serum-supplemented media. Additionally, compared to liposomes that remained uncross-linked, the reduced fluidity of the lipid bilayer cross-linked after chitosan adsorption should limit separation of the hydrophobic chains of the chitosan molecules from the outer leaflet.

In consideration of differences in initial binding stoichiometry in conjunction with the percent desorbed, the molar amount of chitosan adsorbed per liposome after incubation in

dx.doi.org/10.1021/la500412r | Langmuir 2014, 30, 3697−3704

serum further demonstrates the advantage of the sequential adsorption and cross-linking processes (Figure 4b). Here, unlike Figure 2, the glucosamine binding stoichiometry is stated per total lipid content rather than those in the outer leaflet since a population of liposomes was likely ruptured during the incubation period. Uncross-linked liposomes initially presented the same amount of DTPA-chitosan-g-C_{18} adsorbed as liposomes cross-linked after chitosan adsorption. However, due to differences in stability, the amount of glucosamine units that remained bound to the uncross-linked liposome after an hour was almost half of that remaining on the cross-linked liposome. Moreover, in comparing liposomes cross-linked before or following adsorption of modified chitosan, the cross-linking reaction after adsorption represented a 4-fold increase in the amount adsorbed after 1 h due to differences in initial binding stoichiometry as well as stability. The same trends were observed at high concentrations of serum, further highlighting the potential of the cross-linked liposomes to enhance stability under stressed conditions (Figure S2, Supporting Information).

3.4. Magnetic Resonance Contrast Enhancement by Coated Liposomes. To load gadolinium on the liposome surface, liposomes coated with DTPA-chitosan-g-C_{18} were titrated with gadolinium until all DTPA binding sites were saturated, as confirmed by colorimetric complexation with xylenol orange. Xylenol orange serves as an indicator that changes color from yellow to pink, corresponding to a shift in absorbance maxima from 433 to 573 nm, in the presence of unchelated gadolinium.[25] After incubation in serum-supplemented media for 1 h, the amount of gadolinium present per lipid dose, as determined by ICP-OES, was nearly 4-fold greater in the case of liposomes cross-linked after DTPA-chitosan-g-C_{18} adsorption, compared to those cross-linked prior (Figure 5a). The result was consistent with observations of chitosan binding stoichiometry and stability. The chelation of gadolinium by DTPA-chitosan-g-C_{18} was not affected by the presence of serum, as no free gadolinium was detected by the xylenol orange assay, even after 3 days of incubation of the saturated chitosan fastener in serum.

MR phantom images of the liposomes after serum exposure were then acquired to demonstrate the beneficial effects of loading chitosan onto liposome surfaces before lipid bilayer cross-linking. For any given lipid concentration, the liposomes cross-linked prior to coating with DTPA-chitosan-g-C_{18} exhibited the lowest MR signal intensity (Figure 5b). By contrast, the signal intensity was greatest in the case of liposomes cross-linked after DTPA-chitosan-g-C_{18} adsorption. The results can be attributed to the higher concentration of gadolinium per sample as a result of the differences in retention of bound chitosan.

Finally, to further verify that differences in MR signal intensity were due solely to differences in gadolinium concentration rather than molar relaxivity, it was necessary to calculate the relaxivity for the three conditions by linear regression of eq 3:

$$R_1 = R_{1,\text{water}} + r_1[\text{Gd}] \tag{3}$$

where R_1 is the relaxation rate of the phantom $(1/T_1)$, $R_{1,\text{water}}$ is the relaxation rate of water, [Gd] is the concentration of gadolinium, and r_1 is the molar relaxivity of the contrast agent.

The r_1 normalized to gadolinium concentration was compared across the three fabrication processes, as was the lipid-based relaxivity calculated per lipid dose (Figure 5c). As expected, liposomes cross-linked after adsorption of DTPA-chitosan-g-C_{18} had the highest relaxivity per lipid. By contrast, the molar relaxivity per gadolinium concentration was similar across all formulations (Figure 5c). These results confirm that the higher gadolinium loading per liposome due to the

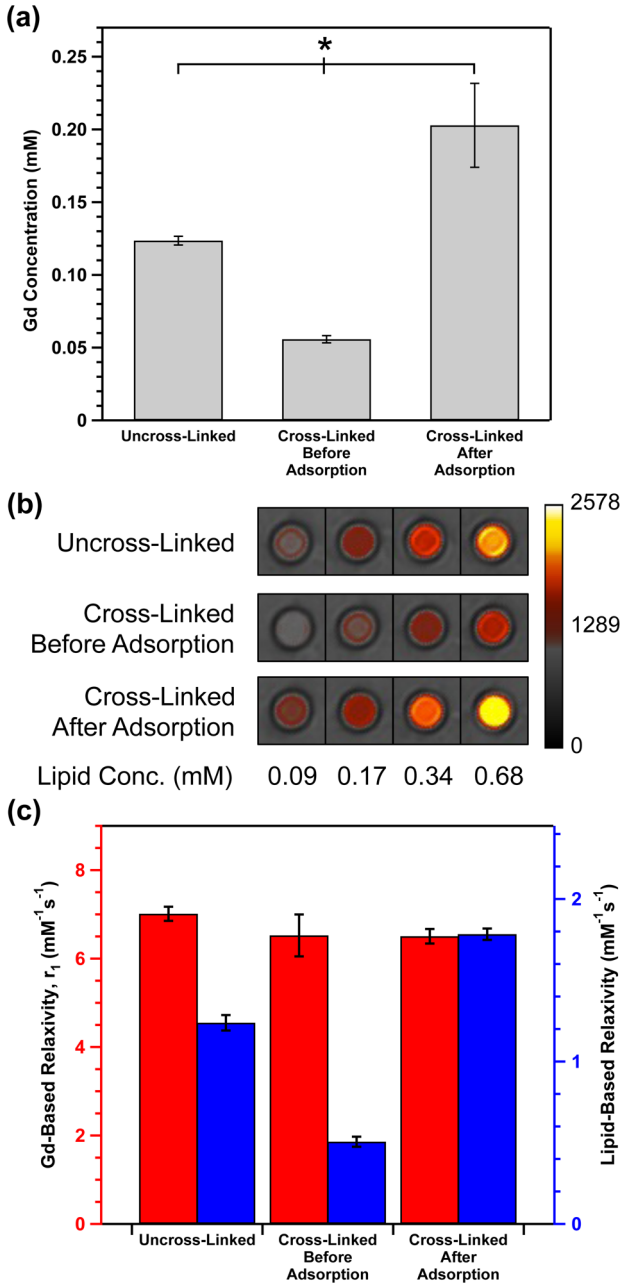

Figure 5. Analysis of gadolinium loading and subsequent MR signal enhancement. (a) ICP-OES analysis of the gadolinium retained in 0.68 mM lipid suspensions after incubation in serum-supplemented media. Values are the average of three replicates shown with error bars as standard deviation. An asterisk (*) represents statistical significance among all conditions (*$p < 0.05$). (b) Pseudocolored MR image of uncross-linked liposomes, and those cross-linked either before DTPA-chitosan-g-C_{18} adsorption or after (TI = 1250 ms). The concentration series is shown per lipid dose, and coloration represents signal intensity values. (c) Gadolinium-based molar relaxivities (red bar) and lipid-based molar relaxivities (blue bar) for the three liposome samples. Error bars represent standard deviation of the fit parameter.

dx.doi.org/10.1021/la500412r | Langmuir 2014, 30, 3697−3704

enhanced binding stoichiometry and retention of the modified chitosan was responsible for the elevated MR contrast.

We therefore propose that the high loading of gadolinium makes the liposomes cross-linked after chitosan adsorption superior for biomedical imaging and, in particular, both active and passive targeted imaging. With the 4-fold increase in loading after incubation in serum, only one-fourth of the number of liposomes would be required to accumulate at a target site to provide a given T_1 relaxation rate, compared to liposomes cross-linked before chitosan adsorption. Alternatively, the signal at the target site would be greatly enhanced for any specific quantity of accumulated liposome. Furthermore, liposomes could be processed within a size range suitable for their application prior to chitosan adsorption. We suggest that this modular method of assembly will not be dependent on liposome size.

To further improve the MR signal of the gadolinium-loaded liposome, the degree of substitution of DTPA to chitosan could be increased to augment the loading of gadolinium. Additionally, the number of alkyl chains per molecule could be increased to provide further binding stability. As liposomes are commonly used as drug carriers, we believe that cross-linking of the bilayer may reduce release rates of molecular cargoes loaded into the liposome, as others observed with various cross-linkable liposome systems.[26,27] Such kinetic effects would have to be considered for each specific application. Strategies for stabilization of micro- or nanoparticles will be critical for the development of future diagnostics or treatments that must remain stable until reaching their target site after injection. In this way, the system described in this study will be useful for a broad range of applications using functionalized liposomes.

4. CONCLUSION

This study demonstrates a strategy to stabilize liposomes coated with a gadolinium-carrying chitosan fastener under physiological conditions. The system consisted of liposomes made from cross-linkable $DC_{8,9}PC$ lipids, and the chitosan modified with a hydrophobic anchor and gadolinium chelate, DTPA-chitosan-g-C_{18}. In particular, liposomes that were cross-linked after DTPA-chitosan-g-C_{18} adsorption were able to retain a significantly greater amount of chitosan in the presence of serum than those cross-linked prior to incubation with chitosan. Thermodynamic analysis addressed that the dependency of association stability on the process is likely due in part to the enhanced insertion of hydrophobic alkyl chains into the lipid bilayer coupled with reduced fluidity after cross-linking of lipids. As a result, the liposome cross-linked after chitosan adsorption loaded a larger amount of gadolinium and dramatically enhanced MR signal per dose of liposome than that cross-linked before chitosan adsorption. Overall, this strategy of stabilizing a polymeric fastener to liposome surfaces can be readily applied to any variety of functional fasteners that could be destabilized in the harsh environment of in vivo circulation.

■ ASSOCIATED CONTENT

Supporting Information

Stability of liposomes in 50% serum-supplemented PBS and optical images of liposomes before and after cross-linking. This material is available free of charge via the Internet at http://pubs.acs.org.

■ AUTHOR INFORMATION

Corresponding Author

*E-mail: hjkong06@illinois.edu.

Notes

The authors declare no competing financial interest.

■ ACKNOWLEDGMENTS

Funding was provided by the National Institutes of Health (1R01 HL109192 to H.J.K. and Chemistry-Biology Interface Training Grant 5T32-GM070421 to C.E.S.) and The Center for Advanced Study at the University of Illinois.

■ REFERENCES

(1) Torchilin, V. P. Recent Advances with Liposomes as Pharmaceutical Carriers. *Nat. Rev. Drug Discovery* **2005**, *4*, 145−160.

(2) Petersen, A. L.; Hansen, A. E.; Gabizon, A.; Andresen, T. L. Liposome Imaging Agents in Personalized Medicine. *Adv. Drug Delivery Rev.* **2012**, *64*, 1417−1435.

(3) Al-Jamal, W. T.; Kostarelos, K. Liposomes: From a Clinically Established Drug Delivery System to a Nanoparticle Platform for Theranostic Nanomedicine. *Acc. Chem. Res.* **2011**, *44*, 1094−1104.

(4) Litzinger, D. C.; Buiting, A. M. J.; van Rooijen, N.; Huang, L. Effect of Liposome Size on the Circulation Time and Intraorgan Distribution of Amphipathic Poly(ethylene glycol)-Containing Liposomes. *Biochim. Biophys. Acta, Biomembr.* **1994**, *1190*, 99−107.

(5) Chono, S.; Tanino, T.; Seki, T.; Morimoto, K. Uptake Characteristics of Liposomes by Rat Alveolar Macrophages: Influence of Particle Size and Surface Mannose Modification. *J. Pharm. Pharmacol.* **2007**, *59*, 75−80.

(6) Nieh, M. P.; Pencer, J.; Katsaras, J.; Qi, X. Spontaneously Forming Ellipsoidal Phospholipid Unilamellar Vesicles and Their Interactions with Helical Domains of Saposin C. *Langmuir* **2006**, *22*, 11028−33.

(7) Krasnici, S.; Werner, A.; Eichhorn, M. E.; Schmitt-Sody, M.; Pahernik, S. A.; Sauer, B.; Schulze, B.; Teifel, M.; Michaelis, U.; Naujoks, K.; et al. Effect of the Surface Charge of Liposomes on Their Uptake by Angiogenic Tumor Vessels. *Int. J. Cancer* **2003**, *105*, 561−7.

(8) Immordino, M. L.; Dosio, F.; Cattel, L. Stealth Liposomes: Review of the Basic Science, Rationale, and Clinical Applications, Existing and Potential. *Int. J. Nanomed.* **2006**, *1*, 297−315.

(9) Allen, T. M. Ligand-Targeted Therapeutics in Anticancer Therapy. *Nat. Rev. Cancer* **2002**, *2*, 750−63.

(10) Kawasaki, N.; Vela, J. L.; Nycholat, C. M.; Rademacher, C.; Khurana, A.; van Rooijen, N.; Crocker, P. R.; Kronenberg, M.; Paulson, J. C. Targeted Delivery of Lipid Antigen to Macrophages via the Cd169/Sialoadhesin Endocytic Pathway Induces Robust Invariant Natural Killer T Cell Activation. *Proc. Natl. Acad. Sci. U.S.A.* **2013**, *110*, 7826−7831.

(11) Smith, C. E.; Shkumatov, A.; Withers, S. G.; Yang, B.; Glockner, J. F.; Misra, S.; Roy, E. J.; Wong, C.-H.; Zimmerman, S. C.; Kong, H. A Polymeric Fastener Can Easily Functionalize Liposome Surfaces with Gadolinium for Enhanced Magnetic Resonance Imaging. *ACS Nano* **2013**, *7*, 9599−9610.

(12) Kamaly, N.; Xiao, Z.; Valencia, P. M.; Radovic-Moreno, A. F.; Farokhzad, O. C. Targeted Polymeric Therapeutic Nanoparticles: Design, Development and Clinical Translation. *Chem. Soc. Rev.* **2012**, *41*, 2971−3010.

(13) Taira, M. C.; Chiaramoni, N. S.; Pecuch, K. M.; Alonso-Romanowski, S. Stability of Liposomal Formulations in Physiological Conditions for Oral Drug Delivery. *Drug Delivery* **2004**, *11*, 123−128.

(14) Moghimi, S. M.; Szebeni, J. Stealth Liposomes and Long Circulating Nanoparticles: Critical Issues in Pharmacokinetics, Opsonization and Protein-Binding Properties. *Prog. Lipid Res.* **2003**, *42*, 463−478.

(15) Yuet, P. K.; Blankschtein, D. Effect of Surfactant Tail-Length Asymmetry on the Formation of Mixed Surfactant Vesicles. *Langmuir* **1996**, *12*, 3819−3827.

(16) Lin, C.-M.; Li, C.-S.; Sheng, Y.-J.; Wu, D. T.; Tsao, H.-K. Size-Dependent Properties of Small Unilamellar Vesicles Formed by Model Lipids. *Langmuir* **2011**, *28*, 689−700.
(17) Boyer, C.; Zasadzinski, J. A. Multiple Lipid Compartments Slow Vesicle Contents Release in Lipases and Serum. *ACS Nano* **2007**, *1*, 176−182.
(18) MicroCal, LLC. *ITC Data Analysis in Origin—Tutorial Guide*, 5th ed.; MicroCal, LLC: Northampton, MA, 1998.
(19) Ho, J. K.; Duclos, R. I.; Hamilton, J. A. Interactions of Acyl Carnitines with Model Membranes: A ^{13}C-NMR Study. *J. Lipid Res.* **2002**, *43*, 1429−1439.
(20) Meier, M.; Seelig, J. Lipid and Peptide Dynamics in Membranes Upon Insertion of N-Alkyl-Beta-D-Glucopyranosides. *Biophys. J.* **2010**, *98*, 1529−38.
(21) Mertins, O.; Dimova, R. Binding of Chitosan to Phospholipid Vesicles Studied with Isothermal Titration Calorimetry. *Langmuir* **2011**, *27*, 5506−5515.
(22) Fennell, C.; Dill, K. Physical Modeling of Aqueous Solvation. *J. Stat. Phys.* **2011**, *145*, 209−226.
(23) Tanford, C. *The Hydrophobic Effect: Formation of Micelles and Biological Membranes*; Wiley and Sons: New York, 1973.
(24) Liu, S.; O'Brien, D. F. Stable Polymeric Nanoballoons: Lyophilization and Rehydration of Cross-Linked Liposomes. *J. Am. Chem. Soc.* **2002**, *124*, 6037−6042.
(25) Barge, A.; Cravotto, G.; Gianolio, E.; Fedeli, F. How to Determine Free Gd and Free Ligand in Solution of Gd Chelates. A Technical Note. *Contrast Media Mol. Imaging* **2006**, *1*, 184−188.
(26) Guo, C.; Liu, S.; Jiang, C.; Li, W.; Dai, Z.; Fritz, H.; Wu, X. A Promising Drug Controlled-Release System Based on Diacetylene/Phospholipid Polymerized Vesicles. *Langmuir* **2009**, *25*, 13114−13119.
(27) Chen, H.; Torchilin, V.; Langer, R. Polymerized Liposomes as Potential Oral Vaccine Carriers: Stability and Bioavailability. *J. Controlled Release* **1996**, *42*, 263−272.